

THE MORPHOLOGICAL INSTABILITY OF A SOLID-LIQUID INTERFACE INDUCED BY SOLID-STATE DIFFUSION

E. Rabkin, B. Straumal, and W. Gust

Max-Planck-Institut für Metallforschung and Institut für Metallkunde, Seestr. 75,
D-70174 Stuttgart, Germany

Abstract

The dissolution of a solid metal in the melt of a metal with a lower melting temperature is investigated for the case of an Fe-7 at.%Si monocrystal dissolving in a Sn melt. The molten Sn penetrates into the monocrystal by an isolated from each other filled with the melt inclusions with an unusually high velocity, which is at least an order of magnitude higher than follows from the volume diffusion equation. Electron probe microanalysis of the compositional distribution in the penetration zone has been performed. A thermodynamic analysis of the phenomenon is presented.

Acknowledgements. The financial support of the Volkswagen Foundation is greatly acknowledged. E.R. wish to thank the Alexander-von-Humboldt Foundation for their support.

Solid→Solid Phase Transformations
Edited by W.C. Johnson, J.M. Howe, D.E. Laughlin and W.A. Soffa
The Minerals, Metals & Materials Society, 1994

Introduction

It is well-known that during the interdiffusion process in concentrated ternary alloys two-phase areas with intermediate phase precipitates can be observed in the diffusion zone [1]. However, the possibility of complex nonplanar interface morphologies in the diffusion zone has been demonstrated recently for binary or quasi-binary systems [2,3]. It has been shown that during diffusion anneal of a thin metallic film on the surface of a polymer the metal penetrates into the polymer as isolated compact clusters [2]. It was found [3] that liquid Ni penetrates along the grain boundaries in pure W not only as a continuous layer, but also in the form of isolated inclusions. The aim of the present paper is to investigate the phenomenon of the loss of stability of the solid-liquid interphase boundary and the formation of inclusions inside the solid. For this sake, we have chosen the Fe(Si) monocrystal - molten Sn system. The use of a monocrystal allows us to exclude the disturbing influence of grain boundaries. There are two reasons for choosing Sn: (1) no intermediate intermetallic phases are formed in the Fe-Sn system above 910°C, and (2) the solubility of Sn in the Fe-based solid solution is high enough to allow electron microprobe measurements in the diffusion zone [4].

Experimental

The Fe-7 at.%Si alloy was produced from Fe of 99.99% purity and Si of 99.999% purity. An Fe-7.at.% Si polycrystalline rod was used to grow a cylindrical <001> single crystal by the electron beam zone floating technique [5]. The 1.5x3x10 mm sample was then cut from the as-grown single crystal. After cutting, the sample was mechanically and chemically polished. A layer of Sn of 99.999% purity was then applied to the sample by immersion into a Sn melt under such conditions that the thickness of the Sn layer after immersion was about 1 mm. The sample was evacuated in the silica ampoule and placed in a furnace with a temperature of 964 °C for 20 min. The temperature of the ampoule increased from room temperature to the desired value of 964 °C within about 10 min, after which it was held constant for 10 min. After annealing, the ampoule was quenched into water, and the sample was prepared for light microscopy (LM) and electron probe microanalysis (EPMA) by standard methods. The EPMA measurements were carried out by wavelength dispersive analysis on a JEOL 6400 electron probe microanalyzer operated at 15 kV. The intensities of the FeK_α, SnL_α, and SiK_α peaks were determined, and the concentrations of these elements were obtained utilizing a program which applied atomic number, absorption, fluorescence and background corrections.

Results

In Fig. 1a, the sample with its structural features is drawn schematically, and the segments where the EPMA measurements were made, are shown. In Fig. 1b the cross-section of the specimen after slight etching in a 5% HNO₃ solution is shown. Above the interphase boundary between the Fe-based solid solution and the Sn there is an approximately 50 μm wide zone of dark inclusions. The average size of the inclusions as well as the distance between the inclusions increase with the distance from the boundary. On the lower part of the figure dark elongated spots of some phase inside the solidified Sn melt are seen. In Fig. 2 another part of the sample is shown with a higher magnification. It is clearly seen that the inclusions are regularly arranged in rows. In Fig. 1c the concentration profile along the segment 1-1 intersecting a particle in the solid Sn is shown. The composition in the middle of the particle is about 50 at.% Sn and 50 at.% Fe, which corresponds to the intermetallic phase FeSn which is stable up to 770 °C. No further intermetallic phases in the solidified Sn melt were found, which is an indication of a high cooling rate. In Fig. 1d the concentration profiles measured in the Fe-based solid solution along the segment 2-2 parallel to the interphase boundary are shown. One cannot determine the exact Sn concentration in the inclusions because the size of the interaction zone of the electron beam during EPMA is comparable with the size of an inclusion. The best estimation of the composition inside the inclusion should therefore be taken from the EPMA values for the widest

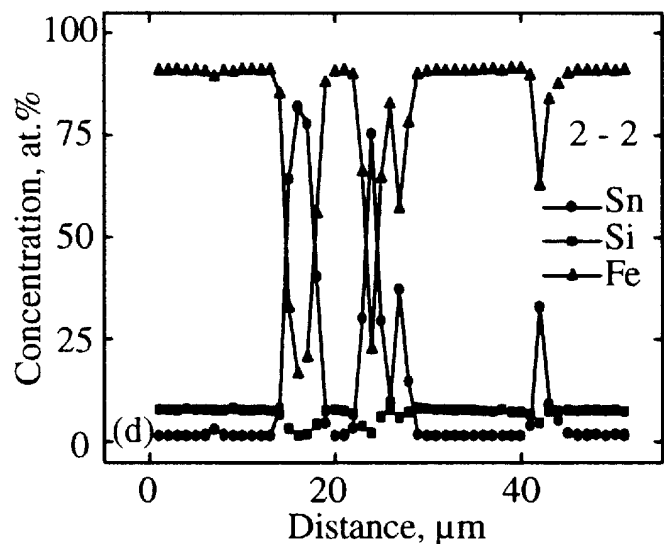
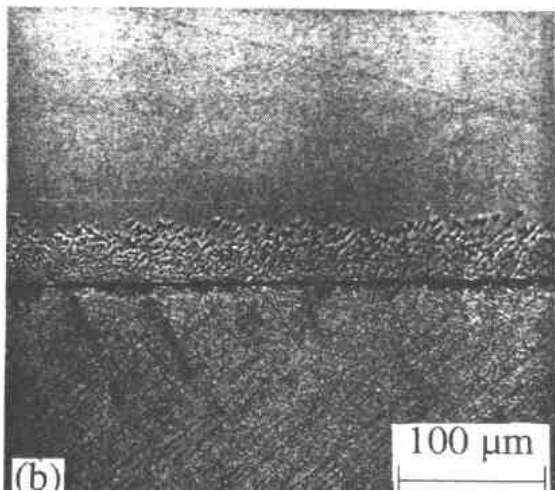
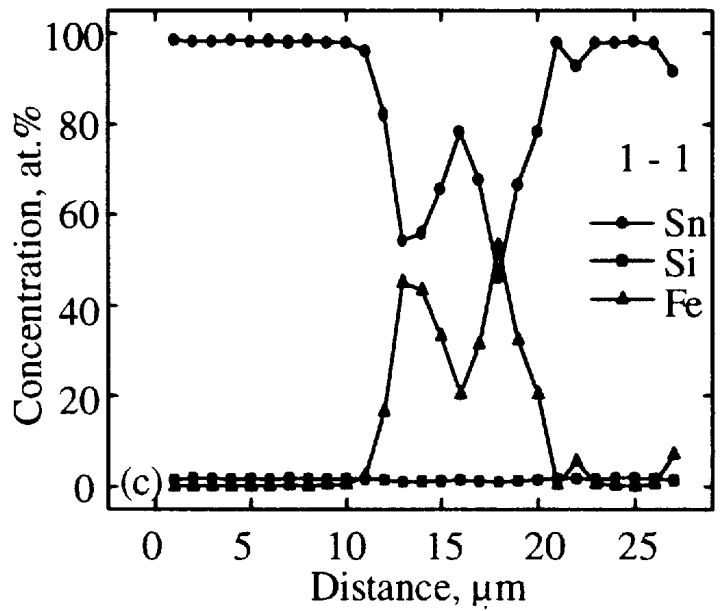
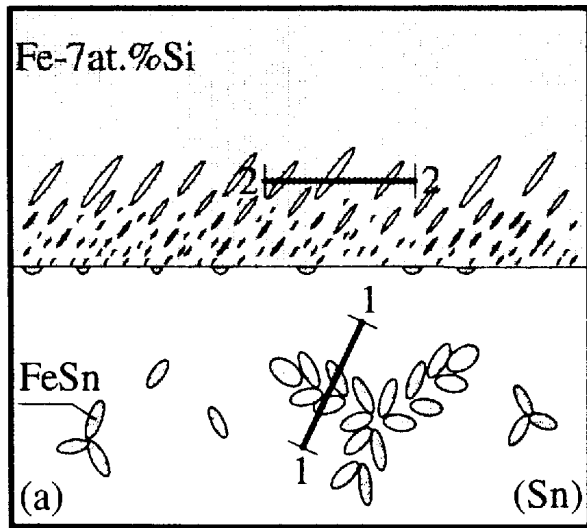


Fig. 1. The schematic diagram of the microstructure (a) and the cross-section (b) of an Fe-7 at.% Si monocystal after interaction with liquid Sn at 964 °C. The EPMA measurements of the element distribution along the trajectories 1-1 (c) and 2-2 (d) are also shown.

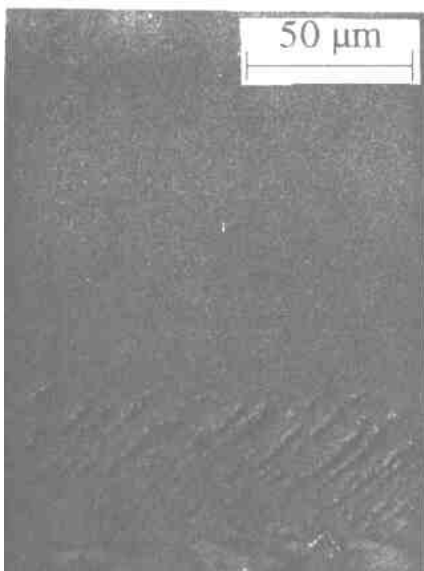


Fig. 2. Cross-section of a sample showing the regular arrangement of Sn-rich inclusions. The interphase boundary between Fe(Si) and Sn lies in the (001) plane.

inclusion. Obviously, this is for the first peak in Fig. 1d where approximately 18 at.% Fe, 82 at.% Sn and 0 at. % Si present. The concentration of Sn in the surrounding bulk is approximately constant (1.5 at.% Sn).

Discussion

The Fe(Si) - Sn system

The concentration of Sn (1.5 at.%) and Si (7 at.%) in the Fe-based solid solution around the inclusions is far below the solubility limits of the Fe-Sn and Fe-Si systems at the temperature studied (9.0 and 28.2 at.%, respectively). Therefore, the supersaturation of the solid solution, which leads to the precipitation in the diffusion zone in concentrated ternary alloys, is excluded in our case as we are dealing with a quasi-binary system [1]. The composition of the material inside the inclusions differs from that given by the equilibrium Fe-Sn phase diagram at 964 °C: 9.0 at.% Sn and 92 at. % Fe. This may be connected with any of the following three factors: (1) the size of the widest inclusion studied is comparable with the resolution limit of EPMA, (2) the thermodynamic equilibrium corresponding to the phase diagram is not reached during the dissolution and diffusion process, or (3) the addition of Si changes the solubility limits considerably. However, in all of the above cases the above composition corresponds to the high temperatures, and the formation of inclusions during the quenching as a result of the decomposition of the supersaturated solid solution is excluded (at low temperatures the liquid phase contains practically 100 at.% of Sn). Let us estimate the size of the diffusion zone formed after a 10 min anneal at 964 °C. The chemical interdiffusion coefficient of Sn in the Fe-5 at.% Si alloy has been measured [6]. Using the Arrhenius parameters from this work one can estimate the interdiffusion coefficient for our case ($1.2 \times 10^{-13} \text{ m}^2/\text{s}$). This corresponds to an average size of the diffusion zone of about 8 μm . That is about one order of magnitude lower than the observed width of the zone with the inclusions (about 50 μm , see Fig. 1). The distribution of the inclusions also does not correspond to those expected from a consideration of the interdiffusion process. The volume fraction of the inclusions does not depend on the depth below the interface and has a value of approximately 20%, while from the consideration of the interdiffusion profile the volume fraction of the inclusions should fall continuously with the depth from a maximal value near the interphase boundary. Therefore, some mechanism in addition to the bulk interdiffusion should be involved in the formation of the inclusions and their transport inside the solid.

Thermodynamic considerations

We will consider the solid-liquid interface to have the excess specific energy γ . Atoms from the liquid phase diffuse into the solid metal and form a solid solution. The atomistically sharp interface together with the diffusion zone can be defined as a generalized interface. Its excess specific energy Γ can be defined using the ideal solution approximation by the equation

$$\Gamma = \gamma + RT\rho_m d \{c_o \ln c_o + (1 - c_o) \ln(1 - c_o)\} \quad (1)$$

where c_o is the average atomic fraction of solute in the diffusion zone, d is the average depth of the diffusion zone, ρ_m is the molar density of the solid, R is the gas constant and T is the absolute temperature. If d or c_o are large enough, Γ can be negative due to the contribution of the second term in Eq.(1). The negative sign of the interface excess energy means the instability of such an interface against an increase of its area. It is the same situation as in the case of superconductors of kind II. The calculation of the excess energy of the interface between the normal and superconducting phases gives a negative value for such superconductors [7]. Physically, it means that a spontaneous penetration of the normal phase into the superconducting one by vortexes occurs. In complete analogy with this phenomenon from the superconductivity, the liquid phase penetrates into the solid metal in order to increase the total

area of the solid-liquid interphase boundary and decrease the free energy of the whole system. The same driving force is responsible for grain boundary migration in the diffusion induced grain boundary migration (**DIGM**) process. We will demonstrate now using the Fe-Cu system as an example that the Γ value can indeed be negative. At 1398 K the values $\gamma \approx 0.43 \text{ J/m}^2$ [8] and $c_0 \approx 0.08$ [4] hold true. From Eq.(1) it can be shown that for $d \geq 1 \text{ nm}$ the Γ value becomes negative. Therefore, when the diffusion zone has reached a thickness of about three to four interatomic distances the free energy of mixing during solid solution formation is already high enough to compensate for the excess energy of the interface. This thermodynamic consideration does not say anything, however, about the possible mechanism of the interface instability development and the pore formation. We will consider below two possibilities.

1. The coherency strain driving force. Srolovitz [9] has shown that the surface of a homogeneously stressed solid is unstable with respect to a periodic perturbation caused by surface diffusion. At a later stage of instability development, thin narrow channels can be formed at the surface [10]. Such channels may later develop into the elongated inclusions, which are clearly seen in Fig. 1b. The reason for such behavior is the stress concentration at the tips of the channels, which let them grow and increase the surface energy. Srolovitz [9,10] has found the relationship between γ , the Young modulus E , the wavelength of instability λ and the homogeneous tensile stress σ , at which the instability develops:

$$\sigma > 1.88 \sqrt{\frac{\gamma E}{\lambda}}. \quad (2)$$

Assuming the value of γ to be that of the Fe-Cu system (0.43 J/m^2), taking from the literature $E \approx 152.3 \text{ GPa}$ [11] and estimating from Fig. 1b the value of λ to be about $10 \mu\text{m}$, we find that stresses higher than 150 MPa are needed in order to induce the instability. Such stresses could be caused by the coherency strain in the penetration zone, which arises due to the concentration dependence of the alloy's lattice parameter. The stress induced by the coherency strain in an isotropic material is given by the equation

$$\sigma_{coh} = \frac{Es^2 \Delta c^2}{1 - \nu} \quad (3)$$

where $s = d \ln a / dc$, a being the lattice parameter of an alloy with the concentration c , and Δc is the difference in the concentration of Sn atoms near the inclusion and far from it. For the Fe-Sn alloy, $s \approx 0.23$ [12] and $\Delta c \approx 7.5 \text{ at.}\%$ (Sn concentration of $9 \text{ at.}\%$ in accordance with the Fe-Sn phase diagram is accepted as the Sn concentration in the solid solution near the inclusion, the concentration far from the inclusion being $1.5 \text{ at.}\%$, see Fig. 2d). Then, from Eq.(3) $\sigma_{coh} \approx 60 \text{ MPa}$, which is lower by a factor of two than stresses necessary for the instability development. However, taking into account some uncertainty in the values of the parameters used, the coherency strain energy could provide a substantial driving force for the instability development, but it should be noted that the value of the parameter s for the Fe-Sn system is very high when compared with that for the other Fe-metal systems [12]. Therefore, the generality of the coherency strain driving force for the instability development is problematic, contrary to the conclusion of [13], where the solid-liquid interface instability has been observed during liquid phase sintering of Mo-Ni alloys.

2. Another reason for the instability development can be the fact that the dissolution of the Fe-Si crystal in the Sn melt is an interface-controlled process. The importance of a finite interface mobility in surface phenomena has recently been pointed out by Cahn and Taylor [14]. We have shown [15] that the interface-limited steady-state dissolution of a crystal in the melt may be accompanied by the loss of stability of the solid-liquid interface if the jump frequencies of the solute atoms across the interface is higher than that of the matrix atoms. We will estimate the

corresponding frequencies by the bulk self- and tracer diffusion coefficients D_{Fe} and D_{Sn} , respectively [16]: $D_{\text{Fe}} \approx 1.4 \times 10^{-14}$ m²/s and $D_{\text{Sn}} \approx 1.0 \times 10^{-13}$ m²/s. Therefore, the mobility of Sn atoms is higher than Fe ones, and if the same is true for the interface, the instability can develop. More experiments are needed in order to decide between two proposed explanations.

References

1. J. Philibert, Atom Movements-Diffusion and Mass Transport in Solids (Les Ulis, Les Editions de Physique, 1991), 430-432.
2. R. Willecke, R. Peter, and F. Faupel, "Grenzflächenuntersuchungen an Metall-Polycarbonat-Verbunden" (Paper presented at the DPG-Frühjahrstagung, Münster, Germany, 21 March 1994), 1289.
3. V. Glebovsky, B. Straumal, V. Semenov, V. Sursaeva and W. Gust, "Grain Boundary Wetting in the W-Ni System", Proceedings of the 13th International Plansee Seminar, 1 (1993), 429-441.
4. T.B. Massalski et al., eds., Binary Alloys Phase Diagrams (Materials Park, ASM, OH, 1990), 1774.
5. V.G. Glebovsky, S.I. Moskvina, and V.N. Semenov, "Growing Techniques and Structure of Nb Bicrystals," J. Crystal Growth, 59 (1982), 450-454.
6. E.I. Rabkin, V.N. Semenov, L.S. Shvindlerman and B.B. Straumal, "Penetration of Tin and Zinc Along Tilt Grain Boundaries 43° [100] in Fe-5 at.% Si Alloy: Premelting Phase Transition?" Acta metall. mater., 39 (1991) 627-639.
7. A.A. Abrikosov, Introduction in Theory of Metals (Nauka, Moscow, 1987), 318.
8. W. Missol, Energies of Interfaces in Metals (Katowice, Slask, 1975), 120.
9. D.J. Srolovitz, "On the Stability of Surfaces of Stressed Solids", Acta metall., 37 (1989), 621-625.
10. W.H. Yang and D.J. Srolovitz, "Cracklike Surface Instability in Stressed Solids", Phys. Rev. Lett., 71 (1993), 1593-1596.
11. C.J. Smithells, ed., Metals Reference Book (London, Butterworth, 1976), 975.
12. W.B. Pearson, A Handbook of Lattice Spacings and Structures of Metals and Alloys (Oxford, Pergamon Press, 1967), 633.
13. W.H. Rhee and D.N. Yoon, "The Instability of Solid-Liquid Interface in Mo-Ni Alloy Induced by Diffusional Coherency Strain", Acta metall., 35 (1987), 1447-1451.
14. J.W. Cahn and J.E. Taylor, "Surface Motion by Surface Diffusion", Acta metall. mater., 42 (1994), 1045-1063.
15. E. Rabkin, B. Straumal, and W. Gust, to be published in Interface Science.
16. H. Mehrer, ed., Diffusion in Solid Metals and Alloys, Landolt-Börnstein, New Series III/26, (Berlin, Springer-Verlag, 1990), 49, 129.